Constraints-Based Modeling Enables Successful Development of a Welding Electrode Specification for Critical Navy Applications

A novel modeling approach substantially reduces risk in developing a high-performance welding electrode specification for critical U.S. Navy applications

BY K. SAMPATH

ABSTRACT. An innovative constraints-based modeling approach was used to successfully specify the chemical composition range for advanced consumable electrodes intended for gas metal arc welding (GMAW) of high-strength steels for critical U.S. Navy applications. Initially, various U.S. Navy requirements for advanced consumable electrodes were converted into a set of constraints that related chemical composition of steels to certain metallurgical characteristics with appropriate numerical ranges. The metallurgical characteristics and their numerical ranges, in turn, were used to identify critical elements for compositional control, and to specify the compositional ranges for the individual alloy elements. Subsequently, a 2^3 factorial design of experiments was used to develop a batch of welding electrodes, and limited experiments were carried out to evaluate the performance of the welding electrodes. Results showed that two of the eight electrodes met or exceeded ER-100S requirements, while one of the eight electrodes met or exceeded ER-120S requirements. Additional weld evaluations performed over a much wider welding operational envelope using one of the eight electrodes provided weldments with acceptable weld mechanical properties for ER-100S over the entire range of welding conditions. Thus, use of the constraints-based modeling approach greatly reduced the risks inherent in developing electrode specification, while allowing one to meet or exceed U.S. Navy requirements at minimal cost and schedule, thereby validating the exceptional utility of this novel modeling approach.

Background

High yield (HY) and high-strength low-alloy (HSLA) type steels with a minimum yield strength of 80 or 100 ksi are used extensively in U.S. Navy ship and submarine construction (Ref. 1). Commercial applications for these high-performance steels include off-highway vehicles, bridges, pressure vessels, storage vessels, etc.

The HY steels were developed in the 1960s and exhibit a tempered martensitic microstructure. The HY-80 and HY-100 steels are characterized by a high carbon content (Ref. 2) ranging from about 0.12 to 0.20 wt-% (percent by weight). Hydrogen-assisted cracking (HAC) in the weld heat-affected zone (HAZ) is a serious issue in the welding of these high-strength structural steels with a high carbon content.

These steels show a high potential to form twinned martensite and solid-state cracking in the HAZ when the following conditions are simultaneously present: 1) a source of dissolved hydrogen; 2) high residual tensile stress distribution; 3) a temperature range that did not allow significant solid-state diffusion of atomic hydrogen from the steel; and 4) a time delay following welding that allowed atomic hydrogen to accumulate at internal "flaws" in the steel, thereby leading to HAC. The HY steels require the application of preheat, interpass, and occasionally post soak temperature controls during welding to reduce the occurrence of HAC in the weld HAZ. These additional operations increase fabrication cost, produce considerable production delays, and increase welder discomfort. It is estimated that elimination or substantial reduction in temperature control during welding could save about $10 million in the construction of an aircraft carrier and $15 million in the construction of a submarine in material, labor, and lost productivity, irrespective of the type of arc welding processes used.

Currently, various U.S. shipyards employ the GMAW process as the preferred fabrication process for constructing several ship structures, and primarily use Ar-5%CO_2 as weld shielding gas. AWS A5.28, *Specification for Low-Alloy Steel Electrodes and Rods for Gas Shielded Arc Welding* (Ref. 3), recommends ER-100S and ER-120S welding consumables for joining HY-80 and HY-100 steels. Table 1 specifies the chemical composition range and mechanical property requirements for ER-100S and ER-120S GMAW consumable electrodes. These electrodes often exhibit a carbon content in excess of 0.05 wt-%. Consequently, these welding consumables also require significant preheat to reduce the occurrence of HAC in the weld metal (Ref. 4).

High-strength low-alloy steels were developed in the 1980s in an effort to reduce fabrication costs (Ref. 1). In contrast to the HY steels, the HSLA-80 and HSLA-100 steels (Ref. 5) have a lower carbon content (0.07 wt-% maximum) and exhibit a ferritic and a bainitic microstructure, respectively. Unlike the martensitic microstructure, the ferritic and bainitic microstructures exhibit little or no susceptibility to HAC. Because of their low susceptibility to HAC, HSLA-80 and HSLA-100 steels require much less stringent preheating controls compared to the corresponding grade of HY steels, thereby offering a huge potential for low-cost fab-

KEYWORDS

Hydrogen-Assisted Cracking (HAC)
Gas Metal Arc Welding (GMAW)
HSLA-80 and HSLA-100 Steels
HY-80 and HY-100 Steels
Carbon Equivalent Number (CEN)
Charpy V-Notch (CVN)
ER-100S and ER-120S Electrodes
Constraints-Based Modeling

K. SAMPATH is a Technology/Business Consultant in Johnstown, Pa.

Table 1 — Chemical Composition Ranges and Mechanical Property Requirements

	AWS A5.28 Specification	
Element	ER 100S	ER 120S
Carbon	0.08	0.10
Manganese	1.25–1.80	1.40–1.80
Silicon	0.20–0.55	0.25–0.60
Phosphorus	0.010	0.010
Sulfur	0.010	0.010
Nickel	1.40–2.10	2.0–2.80
Chromium	0.30	0.60
Molybdenum	0.25–0.55	0.30–0.65
Vanadium	0.05	0.03
Titanium	0.10	0.10
Zirconium	0.10	0.10
Aluminum	0.10	0.10
Copper	0.25	0.25
Other Elements, Total	0.50	0.50
Iron	Balance	Balance
Mechanical Property		
Tensile Strength (ksi)	100	120
Yield Strength (ksi)	88	105
Elongation (%)	16	14
Minimum CVN at 0°F (ft-lb)	—	—
Minimum CVN at –60°F (ft-lb)	50	50

rication of very large structures.

However, HSLA-80 and HSLA-100 steels are currently fabricated with ER-100S and ER-120S solid wire electrodes used for GMAW of HY-80 and HY-100 steels. Since the currently available ER-100S and ER-120S solid wire electrodes require preheat and interpass controls, and post soak temperature control for ER-120S, their use precludes the full economic advantages of HSLA steels (Ref. 6). For the foregoing reasons, there is an economic need for developing advanced consumable, bare, solid-wire electrodes for GMAW of HSLA-80 and HSLA-100 steels.

As the prime user, the U.S. Navy has identified that the candidate advanced GMAW consumables for high-strength steels should exhibit the following characteristics: 1) eliminate or substantially reduce the need for preheat controls; 2) show adequate resistance to HAC; 3) meet or exceed the mechanical property requirements of the existing ER-100S and ER-120S electrodes; 4) allow welding over a broad operational envelope in terms of plate thickness, welding position, and weld energy input; and 5) show minimal variation in weld mechanical properties (especially yield strength) when welded over a broad operational envelope.

Objectives

The present work describes an innovative constraints-based modeling approach that proved quite efficient in developing a specification for consumable, bare, solid-wire electrodes for GMAW of HSLA-80 and HSLA-100 steels that met or exceeded the above U.S. Navy requirements.

A U.S. General Accounting Office report (Ref. 7) has quoted that "only 39% of (U.S. Government) specification parameters were supported by historical data and less than 5% of the parameters were supported by test data," thereby strongly endorsing a need for strengthening the specification development and approval process. In this context, the constraints-based modeling effort was also aimed at directly strengthening this vital process.

Constraints-Based Modeling

The constraints-based modeling approach uses the following two key principles:

1) Consolidate prior and perceived knowledge into a coherent set of mutually inclusive constraints that meet specific requirements; and
2) Use the set of constraints to formulate controlled experiments that would limit the experimental space, while reducing inherent risks, thereby allowing one to reach beyond the consolidated knowledge in developing novel, low-cost, low-risk solutions to overcome persistent materials (processing and fabrication) issues.

Under this modeling approach, initially the various U.S. Navy requirements for ER-100S and ER-120S electrodes (i.e., minimize the need for preheat and interpass temperature controls, while eliminating sensitivity to HAC, improve welding operational envelope to allow wide variations in weld cooling rate and welding productivity, and increase one's ability to achieve acceptable variations in weld mechanical properties despite wide variations in weld cooling rate) were converted into specific constraints that could be related to the chemical composition of steels through a set of mutually inclusive constitutive equations with appropriate numerical ranges. Each of these constitutive equations obtained from prior art underscores one or more metallurgical characteristics. The respective numerical ranges for the selected metallurgical characteristics were also obtained from an analysis of prior art. Specific numerical ranges were decided based on the possibility to achieve a desirable range of mechanical properties (tensile strength, low-temperature toughness) for both ER-100S and ER-120S electrodes, while improving their weldability in terms of excellent resistance to HAC.

The above metallurgical characteristics and their numerical ranges, in turn, were used to identify critical elements for compositional control, and to specify appropriate compositional ranges for the individual alloy elements. Subsequently, a 2^3 factorial design of experiments was used to develop a batch of welding electrodes.

Limited experiments were used to evaluate the performance of these advanced welding electrodes. Results showed that two of the eight electrodes met or exceeded ER-100S mechanical property requirements, while one of the eight electrodes met or exceeded ER-120S mechanical property requirements. Subsequently, one of the eight welding electrodes was evaluated over a much wider range of welding conditions. Results overwhelmingly supported the underlying metallurgical principles.

The use of the constraints-based modeling approach greatly reduced the risks inherent to developing the electrode specification, while allowing one to meet or exceed U.S. Navy requirements at minimal cost and schedule, thereby validating the exceptional utility of this novel modeling approach.

Model Development

The primary emphasis of the modeling effort was to ensure excellent weldability. For the purpose of this work, weldability was defined as the ability to re-create or retain high-performance base metal microstructure that showed a minimal susceptibility to HAC. As the HSLA-80 and HSLA-100 steels have a low carbon content (0.07 wt-% maximum), exhibit a ferritic and bainitic microstructure, respectively, and show a minimal susceptibility to HAC, one could expect that weld metals with similar characteristics, including desired microstructures, would offer excellent weldability. Based on this premise, the various U.S. Navy requirements were converted into a set of mutually inclusive constraints that enabled one to identify and define appropriate chemical composition ranges for providing high-performance weld metals with a predominantly ferritic or bainitic microstructure and minimal susceptibility to HAC.

A composition having the features of the constraints-based model is comprised of iron (Fe) and specific amounts (in percent by weight) of carbon (C), manganese (Mn), nickel (Ni), chromium (Cr), molybdenum (Mo), silicon (Si), copper (Cu), vanadium (V), niobium (Nb), and boron (B) that concurrently satisfy the following three equations:

B_{50} (°C) = 770 – (270 × C) – (90 × Mn)

Table 2 — Chemical Composition of Bare Wire GMAW Electrodes

No.	C	Mn	P	S	Si	Cr	Ni	Mo	V	Cu	Ti	B	O	N	H
1	0.027	1.51	0.001	0.0019	0.34	0.02	2.52	0.52	0.001	0.001	0.033	0.001	69	6	2.11
2	0.028	1.49	0.001	0.0018	0.37	0.01	2.38	0.99	0.001	0.001	0.031	0.001	47	9	1.51
3	0.028	1.54	0.001	0.0018	0.34	0.01	3.78	0.52	0.001	0.001	0.028	0.001	52	10	2.13
4	0.029	1.5	0.001	0.0018	0.35	0.01	3.73	0.98	0.002	0.001	0.03	0.001	78	6	1.46
5	0.03	1.82	0.001	0.0020	0.34	0.01	2.37	0.52	0.003	0.001	0.029	0.001	76	6	1.63
6	0.029	1.82	0.001	0.0021	0.35	0.01	2.38	0.98	0.003	0.001	0.029	0.001	66	7	1.15
7	0.026	1.82	0.001	0.0022	0.35	0.01	3.77	0.51	0.002	0.001	0.027	0.001	64	6	1.79
8	0.03	1.8	0.001	0.0019	0.33	0.01	3.72	0.99	0.003	0.001	0.025	0.0003	82	4	1.23

Chemical composition (# 1 through 8) is expressed in wt-%. Balance is essentially Fe. Chemical composition determined from vacuum induction melt (VIM) billets.
N, O, and H contents determined from bare solid wire electrodes.
N and O contents are expressed in parts per million (ppm).
H content is expressed in mL/100 g of Fe.
Bare wire size is 0.0625 in. diameter.

$$- (37 \times Ni) - (70 \times Cr) - (83 \times Mo) \quad (1)$$

where the calculated value of B_{50} is 400° to 500°C;

$$M_S\ (°C) = 561 - (474 \times C) - (33 \times Mn) - (17 \times Ni) - (17 \times Cr) - (21 \times Mo) \quad (2)$$

where the calculated value of M_S is 400° to 450°C;

$$CEN = C + A(C) \times \{Si/24 + Mn/6 + Cu/15 + Ni/20 + (Cr + Mo + V + Nb)/5 + 5B\} \quad (3)$$

where $A(C) = 0.75 + 0.25 \tanh [20 \times (C - 0.12)]$, and where the calculated value of CEN is 0.28 to 0.41.

The first equation relates the chemical composition to the B_{50} temperature, i.e., the temperature at which 50% bainite transformation occurs (Ref. 8). Bainite refers to a crystalline structure of considerable toughness, combining high strength with high ductility. Bainite is a transformation product of austenite. Lowering the transformation temperature allows one to refine the grain size of the transformation product, leading to simultaneous increases in both tensile strength and ductility. Based on prior art (Refs. 9, 10), a range of 400° to 500°C for the B_{50} temperature allowed one to match the tensile strength range for ER-100S and ER-120S electrodes.

The second equation relates the chemical composition to the M_S temperature, i.e., the temperature at which martensite transformation starts (Ref. 8). Martensite refers to a very hard but brittle structure of iron and carbon that has a higher susceptibility to HAC. Martensite is also a transformation product of austenite. In other words, both bainite and martensite form only from austenite. One could manipulate this characteristic to design the chemical composition of a high-performance steel. For example, a careful lowering of the M_S temperature below the B_{50} temperature of a steel would allow one to achieve a large volume fraction of bainite than martensite in the resultant microstructure.

Based on the ranges for tensile strength, low-temperature toughness, and resistance to HAC of ER-100S and ER-120S electrodes, the desired range for M_S temperature is approximately 400° to 450°C.

The third equation relates the chemical composition to the carbon equivalent number (CEN), which is often used to distinguish the high-strength structural steels that may require preheating during weld fabrication (Ref. 11). The desired value for CEN of structural steels that may eliminate or substantially reduce the need for preheat and interpass temperature controls ranges from 0.28 to 0.41.

High-Performance Steel Weld Metal

Bainitic steels exhibit high tensile strength (in 135 to 170 ksi range) and good impact toughness at low temperature (Refs. 9, 10). The carbon content of these steels typically ranges from 0.08 up to 0.17 wt-%. These steels contain alloy additions, which retard the high-temperature transformation of austenite to pro-eutectoid or blocky ferrite, and facilitate the transformation to lower bainite at the corresponding bainite-start B_S temperature (the temperature at which bainite transformation occurs). While bainite forms only from austenite, the bainite transformation occurs between the B_S and B_F temperatures (Refs. 9, 10), and for the limited purpose of the current modeling work, the author perceived this transformation to be athermal (i.e., insensitive to cooling rate). In other words, percent bainite formed is dependent primarily on the transformation temperature between B_S and B_F. For example, B_{50} temperature indicates the temperature at which 50% bainite transformation occurs. The B_{50} temperature is midway between the B_S temperature and the B_F temperature. The B_F temperature is normally 120°C below the B_S temperature, and 60°C below the B_{50} temperature.

The bainite transformation is known to show dual characteristics, i.e., under certain conditions, the bainite forms athermally from austenite through a displacive reaction involving a limited diffusion of carbon (Ref. 12), while in certain other situations the bainite may nucleate and grow into austenite exclusively through diffusion control. When the bainite transformation occurs athermally, the quantity of bainite formed at a given temperature between B_S and B_F temperatures can be estimated from the ratio of the difference between B_S temperature and the transformation temperature over 120°C, the latter being the difference between B_S and B_F temperatures. In HSLA-100 steel, wherein the maximum carbon content is limited to 0.07 wt-%, prior work (Ref. 13) has shown the bainite transformation to occur athermally. Differential thermal analysis studies performed on experimental low-carbon, low-alloy bainitic weld metals (Ref. 14) have also shown clear evidence for formation of bainite between B_S and B_F temperatures. For the limited purpose of this modeling effort, the bainite transformation in low-carbon, low-alloy steel weld metal was perceived to be athermal, so one could use the constitutive relationship between chemical composition and B_{50} temperature.

Furthermore, the higher strength bainitic steels exhibit a B_{50} temperature in the range of 420° to 550°C and, in this range, the strength of these steels increases linearly with a decrease in B_{50} temperature (Refs. 9, 10). This relationship provides an additional means to predict strength.

The M_S temperature of these steels is often well below their corresponding B_{50} temperature. Considering that both bainite and martensite are products of austenite, one could readily recognize that a high-strength steel will be free from martensite when the M_S temperature of the steel is below its B_F temperature. Specifically, when the M_S temperature is at least 30°C below the B_{50} temperature, then more than 75% of the weld metal would likely contain bainite. Imposition of this additional constraint to reduce the

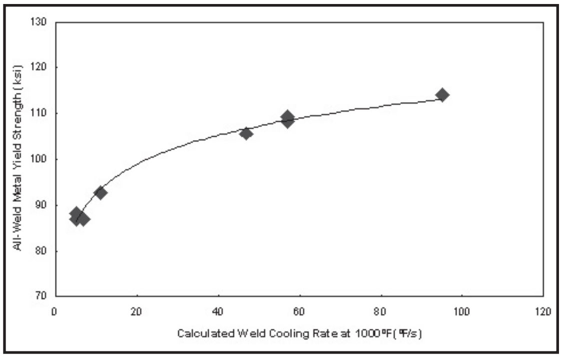

Fig. 1 — Variation of weld metal yield strength with calculated weld cooling rate.

volume fraction of martensite in weld metal to less than 25% can be expected to provide a weld metal with a predominantly bainitic microstructure with the necessary strength, toughness, and resistance to HAC characteristics. Accordingly, a steel with an M_S temperature 30° to 50°C below its B_{50} temperature will have very little martensite, and may exhibit only a limited susceptibility to HAC. As HAC occurs primarily in the presence of a martensitic microstructure, the above constraint provides an additional means to ensure against HAC.

Interestingly, the B_S, B_F, and B_{50} temperatures as well as the M_S and M_F temperatures are all related to the chemical composition of the steel (Ref. 8). Consolidation of this prior knowledge identifies that low-carbon, low-alloy welding electrodes designed to provide weld metal characterized by a B_{50} temperature in the range of 400° to 500°C, and an M_S temperature well below their corresponding B_{50} temperature, would exhibit high strength and acceptable Charpy V-notch (CVN) impact toughness. Furthermore, the athermal nature of the bainite transformation, in this instance as perceived by the author, is likely to permit the use of a wide operational envelope, i.e., large changes in weld heat input conditions may still produce weld metal microstructure with acceptable variations in weld mechanical properties.

Minimize the Need for Preheat

Interestingly enough, the preheat, interpass, and post soak temperature controls necessary to minimize the susceptibility of structural steels to HAC can be also related to the chemical composition of the steels through the CEN equation (Ref. 8). The CEN is expressed as a function of carbon (C), manganese (Mn), nickel (Ni), chromium (Cr), molybdenum (Mo), silicon (Si), copper (Cu), vanadium (V), niobium (Nb), and boron (B) content, in weight percent. In general, as the value of CEN increases, so does the need for increasing the level of preheat, when using a low-hydrogen fusion welding practice.

One could use the CEN equation to assess the relative effects of different alloy elements on the need for preheat. Evidently carbon content has the greatest effect on the CEN. When considering weld metal, a substantial reduction in the carbon content of the welding consumable is necessary to obtain significant reduction in preheat levels. To further reduce the CEN and the sensitivity of weld metals to preheat controls, it is desirable to limit the levels of elements with the highest coefficients in the CEN equation (e.g., boron, chromium, molybdenum, vanadium, niobium) and increase the levels of elements with the lowest coefficients in the CEN equation (e.g., silicon, nickel, copper, and manganese).

Since copper and silicon contribute relatively little to strengthening, and excessive additions may promote fusion zone solidification cracking (especially should the weld metal undergo primary austenitic type solidification), it is preferable that a substantial reduction in carbon content is compensated with appropriate increases in nickel and manganese contents to achieve adequate strength and toughness without impairing the sensitivity to preheat. Excessive increases in nickel content could be expected to stabilize austenite. As austenite has a higher solubility for hydrogen, and eventual transformation of a hydrogen-enriched austenite could potentially lead to HAC, it is desirable to limit excessive increases in nickel content to preclude the occurrence of retained austenite.

Consolidation of this prior knowledge identifies that low-carbon welding electrodes based on a Fe-C-Mn-Ni-Mo system with a CEN ranging from 0.28 to 0.41 (Ref. 15) may meet or exceed U.S. Navy needs.

Low-Temperature Toughness

Besides microstructural control to achieve mechanical property goals, one should also consider the effects of inclusions on achieving minimum low-temperature toughness requirements. Depending on both morphology and size distribution, oxide and nitride inclusions in steel weld metals often decrease weld-metal ductility and in certain extreme situations may also lead to the occurrence of incomplete fusion type weld defects. Therefore, it is desirable to minimize the combined oxygen and nitrogen content, preferably below 550 ppm (Refs. 15, 16). The gas content can be controlled initially through producing melts for wire electrodes using vacuum induction melting practices and subsequently through the application of suitable welding conditions, e.g., a principally inert gas atmosphere, despite the presence of adverse humidity conditions at shipyards.

Thus, a consolidation of the above prior knowledge shows the immense use of the new constraints-based modeling approach for specifying the chemical composition of solid wire electrodes for GMA welding of HSLA steels as it relates to the U.S. Navy requirements (weld operational envelope, and weld strength and toughness properties) with the following metallurgical criteria: B_{50} temperature (the temperature at which 50% bainite transformation occurs), M_S temperature (the temperature at which martensite transformation starts), and combined oxygen and nitrogen content. Concurrently, this approach also relates the need to eliminate or reduce preheat, interpass, and post soak temperature controls with the CEN of the weld metal.

Mutually Inclusive

Using the constraints-based modeling approach, the following metallurgical criteria (Ref. 17) for weld metal were employed in specifying the chemical composition of solid wire electrodes to meet the strength and toughness requirements of ER-100S and ER-120S electrodes, as well as exhibit a reduced sensitivity to preheat:

1) A B_{50} temperature ranging from 400° to 500°C;

Table 3 — Calculated Metallurgical Characteristics of Bare Wire Welding Electrodes

No.	B_{50} Temperature (°C)	M_S Temperature (°C)	Carbon Equivalent Number (CEN)	Combined (O+N) Content (ppm)
1	489	444	0.29	75
2	457	437	0.33	56
3	440	422	0.32	62
4	407	414	0.36	84
5	467	435	0.31	82
6	428	426	0.36	73
7	417	414	0.34	70
8	379	403	0.39	86

Table 4 — GMAW Schedules for Demonstration Weldments

Weld Series	Voltage (Volts)	Current (Amps)	Weld Travel Rate (in./min)	Energy Input (kJ/in.)	Preheat/Interpass Temperature (°F)	Measured Weld Cooling Rate at 1000°F (°F/s)
A	27	310	9	55	60/125	42–44
B	28	340	5	110	60/125	23–24
C	28	340	5	110	275/300	10.8–11.5
Root Pass	25	280	12	35	60/125 or 275/300	—

Table 5 — Mechanical Property Test Results of GMA Welds

	Room-Temperature All-Weld Tensile Test				CVN Impact Test (ft-lb)	
Weld No.	Yield Strength (ksi)	Ultimate Tensile Strength (ksi)	Elongation (%)	Reduction in Area (%)	At –60°F	At 0°F
ER100S	—	100 min	—	—	50 min	—
ER120S	—	120 min	—	—	50 min	—
1A	88.6	102.5	24.0	72.2	44.8	107.4
1B	87.5	99.2	24.5	72.5	73.0	111.6
1C	81.8	96.3	26.5	71.6	51.5	90.8
2A	108.4	116.2	21.4	70.4	60.7	98.6
2B	95.1	108.6	23.5	69.2	26.2*	72.8
2C	88.5	107.4	24.5	71.0	25.2*	66.2
3A	105.7	114.6	22.0	68.9	74.6	102.0
3B	92.6	105.1	23.5	70.9	73.2	112.0
3C	88.3	102.8	24.3	70.6	49.0	95.0
4A	118.3	127.6	20.5	66.7	48.4	74.0
4B	104.4	118.1	22.0	66.4	68.6	90.8
4C	102.2	120.7	21.5	67.4	47.4	89.2
5A	93.8	103.9	23.0	70.2	68.4	108.2
5B	85.6	100.4	25.8	71.0	51.6	98.8
5C	80.2	98.2	24.8	70.3	45.7	100.0
6A	113.3	122.4	21.5	66.8	52.7	76.4
6B	98.5	113.6	23.0	68.4	46.3	90.6
6C	95.9	112.0	24.3	68.6	38.2	99.6
7A	107.2	116.7	20.5	67.4	69.2	89.4
7B	96.2	109.6	23.0	69.3	88.4	109.4
7C	88.3	108.0	24.8	69.1	67.8	107.4
8A	121.2	132.8	20.8	64.9	54.8	75.4
8B	107.3	125.2	21.5	65.5	62.4	95.8
8C	108.2	122.2	23.5	66.4	54.2	86.4

Tensile test results represent an average of 2 tests; CVN impact test results represent an average of 5 tests.
* Visual examination of fractured surfaces showed weld defects.

2) An M_S temperature less than the corresponding B_{50} temperature;
3) A CEN ranging from 0.28 to 0.41; and
4) A combined oxygen and nitrogen content, preferably below 550 ppm.

The above criteria for weld metal chemical composition were then satisfied in a mutually inclusive fashion through a judicious specification of the chemical composition of the solid wire electrodes.

For example, in specifying the chemical composition of the welding electrode and the dependent weld metal, one could remove chromium and significantly reduce the carbon content in the wire electrode (much below the 0.07 wt-% maximum specified for HSLA-100 steel), and thereby reduce the CEN, and substantially minimize the need for preheat controls. These losses in alloy content could be compensated with appropriate increases in nickel and manganese content of the wire electrode to meet the criteria for B_{50} and M_S temperatures, and thereby achieve adequate strength and toughness in the weld metal without impairing its sensitivity to preheat. In contrast, substituting molybdenum in the place of carbon is likely to provide only a minimal decrease in CEN, while substantial additions of molybdenum to reduce CEN may not allow one to meet the B_{50} and M_S temperatures criteria. The interplay of specific elements in simultaneously controlling the calculated B_{50} temperature, M_S temperature, and CEN within desirable ranges can be easily ascertained using an appropriate computer algorithm.

Experimental Evaluation

Electrode Design

Based on the above considerations, a batch of eight solid wire electrodes was prepared (Refs. 17, 18). These eight low-carbon (at about 0.03 wt-%) compositions were based on a 2^3 factorial design, with one low and another high level for manganese (approximately 1.5 and 1.8 wt-%), nickel (approximately 2.5 and 3.8 wt-%), and molybdenum (approximately 0.5 and 1.0 wt-%) and contained other elements such as silicon, phosphorus, and sulfur at some nominal values. As both HSLA-80 and HSLA-100 steels exhibit a higher nickel content than manganese content (Ref. 5), the wire formulations used a higher nickel content, and a relatively lower manganese content in order to minimize difficulties that could possibly occur due to base metal dilution effects. The compositions also included approximately 0.03 wt-% titanium as a deoxidizer, grain refiner, and "nitrogen getter," and thus attempted to control the amount of oxygen and nitrogen in the weld metal. Prior investigation using experimental flux-cored wire electrodes has shown the beneficial effect of titanium addition in controlling weld metal nitrogen content (Ref. 16). Titanium addition also served to refine the weld metal grains.

The actual chemical compositions of the solid wire electrodes were also adjusted using appropriate delta quantities (Ref. 19) to compensate for the loss of alloying elements (particularly manganese) across the arc column. In GMAW, the delta quantities of alloy elements vary with alloy element, shielding gas type, flow rate, and weld energy input. For example, when Ar-5% CO_2 is used as a shielding gas, the delta quantity for carbon is +0.01 wt-%, i.e., one would commonly observe a 0.01 wt-% pickup in the carbon content of the weld metal relative to that of the welding electrode. Likewise, under similar welding conditions, the delta quantity for manganese is –0.2 wt-%, i.e., one would commonly observe a 0.2 wt-% decrease in the manganese content of the weld metal relative to that of the welding electrode. Table 2 shows the melt chemical composition of the solid wire electrodes.

Ingots were produced using the vacuum induction melting (VIM) practice as it allowed a strict control over hydrogen, oxygen, and nitrogen content of the melt. Careful selection of raw materials and vacuum processing were employed to control residual elements such as sulfur and phosphorous. The VIM ingots were subsequently hot rolled and drawn into 0.0625-in.-diameter solid wire electrodes. The wire drawing operation encountered a marginal increase in wear loss in the drawing dies, compared to conventional high-strength steel wire electrodes. An 80% yield was obtained from the starting quantity to the final finish quantity. The solid wire electrodes showed acceptable cast and pitch (helix). Table 3 shows the calculated metallurgical characteristics of the solid wire electrodes based primarily on melt composition.

Demonstration Weldments

Using each of the eight experimental wire electrodes, a set of three demonstration weldments was produced in 1-in.-thick HSLA-100 steel plate using a stringer bead, multipass GMAW technique. The three weldments were designated series A, B, and C (Table 4). The GMAW procedure employed a single- V joint preparation with a 45-deg included angle, a ½-in. root opening with a ½-in.-thick strip permanent backing bar, and 0.0625-in.-diameter solid wire electrodes. The weld test assemblies typically measured 1 × 36 × 36 in. in size. The weldments were produced in the flat position and with nominal restraint.

The same set of welding parameters was used to produce both the root passes and the fill passes in the A-series welds (55 kJ/in. energy input). The root passes of the B- and C-series welds were produced using 35 kJ/in. energy input, while 110 kJ/in. energy input was used to produce the fill passes. In general, the GMAW conditions closely simulated typical shipyard fabrication conditions. These included protective shielding of the weld metal using a principally inert shielding gas (Ar-5% CO_2) at 35 ft^3/h flow rate, and ¾ to 1 in. stickout. The stringer bead, multipass welding technique used 10–15-deg torch lag angle to effectively tie in the weld passes and to produce a desirable overlap between individual weld beads. Consistent with acceptable cast and pitch, all of the experimental wires showed good feeding behavior and minimal weld spatter, which resulted in excellent bead characteristics. The cooling rate at 1000°F of each of the demonstration weldments was measured by plunging a Pt/Pt-Rh thermocouple into the trailing edge of the weld pool of a fill pass at plate midthickness.

Weld Testing

Following the completion of welding and a radiographic examination of the demonstration weldments, room-temperature all-weld-metal tensile tests, and weld metal CVN impact tests (at –60° and 0°F) were performed in the as-welded condition, per MIL-STD-248 using appropriate test specimens. The test results, which included yield strength (YS), ultimate tensile strength (UTS), the percent elongation at failure (EL), the percent reduction of area at failure (RA), and CVN impact results at –60° and 0°F, are summarized in Table 5.

The test results showed the weld metals produced using solid wire electrodes #7 and #8 to meet or exceed the mechanical property requirements of ER-100S, and match/undermatch the yield strength of HSLA-100 steel, and match/overmatch the yield strength of HSLA-80 steel. Additionally, weld metal produced using the wire electrode #8 was found to meet or exceed the mechanical property requirements of ER-120S, and match/undermatch the yield strength of HSLA-100 steel, and overmatch the yield strength of HSLA-80 steel, under all three welding conditions.

Table 6 — Calculated Metallurgical Characteristics of GMA Weld Metals

Weld No.	B_{50} Temperature (°C)	M_S Temperature (°C)	Carbon Equivalent Number (CEN)	Combined (O+N) Content (ppm)
1A–1C	501–502	444–446	0.28–0.29	211–229
2A–2C	462–480	433–438	0.33–0.34	182–211
3A–3C	*446–461*	*421–423*	*0.33–0.34*	216–228
4A–4C	417–437	410–415	0.37–0.38	211–226
5A–5C	487–491	439–442	0.29–0.30	187–196
6A–6C	430–453	421–427	0.36–0.37	130–195
7A–7C	422–432	411–413	0.35	190–203
8A–8C	404–410	403–408	0.38–0.41	192–221

Table 7 — GMAW Schedules for Additional Evaluation

Weld No.	Base Plate	Energy Input (kJ/in.)	Welding Position	Metal Transfer	Preheat Temperature (°F)	Interpass Temperature (°F)	Calculated Weld Cooling Rate at 1000°F (°F/s)
1	HSLA-100	30	Flat	Spray	125	125	95
2	HSLA-100	45	Flat	Spray	150	150	57
3	HY-100	45	Flat	Spray	150	150	57
4	HSLA-100	55	Flat	Spray	60	125	47
5	HSLA-100	110	Flat	Spray	60	125	11
6	HSLA-100	110	Uphill	Pulsed	300	300	7
7	HSLA-100	110	Flat	Spray	275	300	5
8	HY-100	110	Flat	Spray	300	300	5

Table 8 — Mechanical Property Test Results of Additional GMA Welds

Weld No.	Base Plate	Weld Cooling Rate at 1000°F (°F/s)	Room-Temperature All-Weld Tensile Test: Yield Strength (ksi)	Ultimate Tensile Strength (ksi)	Elongation (%)	Reduction in Area (%)	CVN Impact Test (ft-lb): At –60°F	At 0°F
ER-100S	HY-100/HY-80	—	—	100.0	—	—	50 min	—
1	HSLA-100	95	114.0	119.2	19.2	63	86	124
2	HSLA-100	57	108.2	114.8	21.3	68	74	90
3	HY-100	57	109.2	116.2	22.3	67	76	96
4	HSLA-100	47	105.7	114.6	22.0	69	75	102
5	HSLA-100	11	92.6	105.1	23.5	71	73	112
6	HSLA-100	7	87.0	109.0	24.3	72	125	146
7	HSLA-100	5	88.3	102.8	24.3	71	49	95
8	HY-100	5	87.0	102.8	25.8	72	99	129

Tensile test results represent an average of 2 tests; CVN impact test results represent an average of 5 tests.

Model Validation

Details of weld metal chemical compositions are presented in U.S. Patent 5,744,782 (Ref. 20). Table 6 shows the numerical ranges for the calculated metallurgical characteristics of the above GMA weld metals. The results revealed several general trends. First, yield strength of the weld metals increased with CEN. Second, for a given B_{50} temperature, welds produced using higher cooling rates showed a higher strength. Third, for a given M_S temperature, welds produced using higher cooling rates showed a higher strength. Fourth, at a given CEN, the CVN impact toughness increased with increasing weld cooling rates. The above trends were consistent with the known effects of higher weld cooling rate in refining weld metal grain size, and the effects of refined grain size in simultaneously improving both yield strength and low-temperature impact toughness. Fifth, a comparison of the effects of oxygen content and nitrogen content of the weld metals on the CVN impact toughness at 0° and –60°F indicated the beneficial effects of minimal amounts of oxygen and nitrogen in improving weld metal CVN impact toughness.

Table 9 — Proposed Revisions to AWS A5.28 Specification

Chemical Composition

Element	ER 100S Current	ER 100S Proposed	ER 120S Current	ER 120S Proposed
Carbon	0.08	0.08	0.10	0.08
Manganese	1.25–1.80	1.0–2.0	1.40–1.80	1.0–2.0
Phosphorus	0.010	0.010	0.010	0.010
Silicon	0.20–0.55	0.20–0.55	0.25–0.60	0.20–0.60
Sulfur	0.010	0.010	0.010	0.010
Nickel	1.40–2.10	2.0–4.0	2.0–2.80	2.0–4.0
Chromium	0.30	0.30	0.60	0.30
Molybdenum	0.25–0.55	0.30–1.0	0.30–0.65	0.50–1.0
Vanadium	0.05	0.05	0.03	0.05
Titanium	0.10	0.10	0.10	0.10
Zirconium	0.10	0.10	0.10	0.10
Aluminum	0.10	0.10	0.10	0.10
Copper	0.25	0.25	0.25	0.25
Other Elements, Total	0.50	0.50	0.50	0.50
Iron	Balance	Balance	Balance	Balance

Mechanical Property

Tensile/Impact Property	ER 100S Current	ER 100S Proposed	ER 120S Current	ER 120S Proposed
Yield Strength (ksi)	88	82–120	105	105–122
Minimum Tensile Strength (ksi)	100	100	120	120
Minimum Tensile Elongation (%)	16	16	14	15
Minimum CVN at 0°F (ft-lb)	—	80	—	80
Minimum CVN at –60°F (ft-lb)	50	50	50	50

Additional Evaluation

Following the above initial evaluation, welding electrode #3 was used for additional evaluation. A set of eight GMA weldments was produced in 1-in.-thick HSLA-100 and HY-100 steel plates using a wide range of shipyard fabrication conditions. Table 7 shows the GMAW schedule employed for producing weldments for these additional evaluations. Table 7 also shows the calculated weld cooling rates that ranged from 95° to 5°F/s. The weld cooling rates were calculated using the procedure outlined in Ref. 21. As before, following welding, both room-temperature all weld tensile and CVN impact at 0° and –60°F weld mechanical property tests were performed. Table 8 shows the results of the weld metal mechanical property tests.

Figure 1 shows the variation in weld metal yield strength with calculated weld cooling rate. The trend line showed the following statistical relationship, at a r^2 value of 0.99:

$$\text{Yield strength (in ksi)} = 75 \times (\text{Calculated weld cooling rate at } 1000°\text{F/s})^{0.09}$$

At low weld energy input conditions or high weld cooling rates, welding electrode #3 provided weld metals with yield strengths that overmatched the yield strength of the base material. The same electrode, at high weld energy input conditions or low weld cooling rates, provided weld metals with yield strengths that undermatched the yield strength of the base material. The weld metal toughness was exceptionally good in all cases, although weld #7, produced at very high energy input and with HSLA-100 plate, narrowly missed the minimum CVN impact toughness requirement at –60°F. Weld #8 produced under identical welding conditions, but with HY-100 plate instead of HSLA-100 plate, showed exceptional CVN impact toughness properties at –60°F, possibly underscoring the influence of base metal dilution and epitaxial growth effects on weld metal mechanical properties. The ational envelope reflecting a broad range of shipyard welding conditions showed acceptable variation in weld mechanical properties, meeting or exceeding specific U.S. Navy requirements.

Conclusions

1. A constraints-based modeling approach was used to successfully specify the chemical composition of new, advanced solid wire electrodes for GMAW of HSLA-80 and HSLA-100 steels.

2. The metallurgical characteristics of the GMA weld metals and the corresponding all-weld-metal mechanical property test values confirmed the validity and utility of the constraints-based modeling approach in specifying the chemical composition of new, advanced solid wire electrodes.

3. The metallurgical criteria related the strength and toughness requirements of weld metals with the chemical composition of the wire electrodes.

4. The metallurgical criteria also related the need to eliminate or substantially reduce preheat, interpass, and post soak temperature controls with the chemical composition.

5. Solid wire electrodes and welding conditions that provided weld metal characterized by 1) a CEN ranging from 0.33 to 0.41; 2) a B_{50} temperature ranging from 404° to 461°C; 3) an M_S temperature less than the B_{50} temperature; and 4) minimal oxygen and nitrogen content exhibited superior weld mechanical properties, including excellent low temperature toughness when welding HSLA-100 and HY-100 steels over a range of weld energy input and preheat, and interpass temperature controls.

6. The constraints-based modeling approach allowed a better control of materials specification development for high-strength steel welding electrodes, and strengthened the understanding of the effects of weld metal chemical composition on processing (welding operational envelope), microstructure development, and mechanical properties.

Future Work

Based on the above work, and the results of other recent work performed under the auspices of U.S. Navy and commercial electrode manufacturers, the AWS A5 Filler Metal Committee may like to revise the chemical composition ranges specified in A5.28, *Specification for Low-Alloy Steel Electrodes for Gas Shielded Arc Welding*, to reflect these latest advances in the understanding of the relationships among chemical composition, welding conditions, weld microstructure development, and resultant weld mechanical properties of low-alloy high-strength steel weld metals. Table 9 shows the proposed revisions to the chemical composition ranges of the AWS A5.28 Specification. Some of the mechanical property ranges proposed in Table 9 are derived from MIL-E-23765/2E(SH) specification (Ref. 22).

Acknowledgments

The author is pleased to acknowledge Paul W. Holsberg, Charles L. Null, Howard A. Kuhn, and Richard S. Green for their encouragement and support.

References

1. Montemarano, T. W., Sack, B. P., Gudas, J. P., Vassilaros, M. G., and Vanderveldt, H. H. 1986. High strength low alloy steels in naval construction. *Journal of Ship Production* 2(3): 145–162.

2. MIL-S-16216K (SH), *Steel Plate, Alloy, Structural, High Yield Strength (HY-80 and HY-100)*. June 1987.

3. A5.28, *Specification for Low-Alloy Steel Electrodes and Rods for Gas Shielded Arc Welding.* 2005. Miami, Fla.: American Welding Society.

4. Holsberg, P. W., Gudas, J. P., and Caplan, I. L. 1990. Navy's welding research picks up steam. *Advanced Materials & Processes* 138(1): 45–49.

5. MIL-S-24645A (SH), *Steel Plate, Sheet or Coil, Age-Hardening Alloy, Structural, High Yield Strength (HSLA-80 and HSLA-100)*. January 1990.

6. Holsberg, P. W., and Wong, R. J. 1990. Welding of HSLA-100 for naval applications. *Weldability of Materials*. Eds. R. A. Patterson and K. W. Mahin. Materials Park, Ohio: ASM International, pp. 219–239.

7. Navy Ships: Lessons of Prior Programs May Reduce New Attack Submarine Cost Increases and Delays, GAO/NSIAD-95-4, United States General Accounting Office GAO Report to Congressional Requesters. October 1994. p. 7.

8. Steven, W., and Haynes, A. G. 1956. The temperature of formation of martensite and bainite in low-alloy steels. *Journal of the Iron and Steel Institute* 183(8): 349–359.

9. Irvine, K. J., and Pickering, F. B. 1957. Low-carbon bainitic steels. *Journal of the Iron and Steel Institute* 184(12): 292–309.

10. Leslie, W. C. 1981. *The Physical Metallurgy of Steels*. Tokyo, Japan: McGraw-Hill International Book Company, McGraw-Hill, Kogakusha, Inc., pp. 201–205.

11. Yurioka, N., Suzuki, H., Ohshita, S., and Saito, S. 1983. Determination of necessary preheating temperature in steel welding. *Welding Journal* 62(6): 147s–153s.

12. Bhadeshia, H. K. D. H. 2001. *Bainite in Steels*. Institute of Materials, U. K., Second Edition: p. 406.

13. Wilson, A. D. International Steel Group (formerly Lukens Steel Company). Coatesville, Pa.

14. Blackburn, J. M. U.S. Navy, Navy Yard. Washington, D.C.

15. Green, R. S., Sampath, K., Devletian, J. H., Singh, D., Howden, D. G., and Zhang, L. 1993. Filler wire development for GMA welding of HSLA-100 steel. *International Trends in Welding Science and Technology*. Eds. S. A. David and J. M. Vitek. Materials Park, Ohio: ASM International, pp. 359–364.

16. Wong, R. J., and Hayes, M. D. 1990. *The Metallurgy, Welding & Qualification of Microalloyed (HSLA) Steel Weldments.* Miami, Fla.: American Welding Society, pp. 450–489.

17. Sampath, K., Green, R. S., Civis, D. A., Williams, B. E., and Konkol, P. J. 1995. Metallurgical model speeds development of GMA welding wire for HSLA steel. *Welding Journal* 74(12): 69–76.

18. Sampath, K., Green, R. S., Civis, D. A., Dong, H., and Konkol, P. J. 1995. Evaluation of new high performance electrodes for GMA welding of HSLA-100 steel. *High Performance Structural Steels*. Ed. R. Asfahani. Materials Park, Ohio: ASM International, pp. 179–188.

19. Oldland, P. T., Ramsay, C. W., Matlock, D. K., and Olsen, D. L. 1989. Significant features of high-strength steel weld metal microstructures. *Welding Journal* 68(4): 158-s to 168-s.

20. Sampath, K., and Green, R. S. April 1998. U.S. Patent: 5,744,782, Advanced Consumable Electrodes for Gas Metal Arc (GMA) Welding of High Strength Low Alloy (HSLA) Steels.

21. Jhaveri, P., Moffatt, W. G., and Adams, Jr. C. M. 1962. The effect of plate thickness and radiation on heat flow in welding and cutting. *Welding Journal* 41(1): 12-s to 16-s.

22. MIL-E-23765/2E (SH), "Electrodes and Rods — Welding, Bare, Solid, or Alloy Cored; and Fluxes, Low Alloy Steel." April 1994.